Induced Seismicity in Western Canada: Causes and Consequences

David W. Eaton & Thomas S. Eyre
Department of Geoscience – University of Calgary, Calgary, AB, Canada

ABSTRACT
Induced seismicity refers to earthquakes or other seismic events that are associated with human activity. Examples of activities that could cause induced seismicity are impoundment of surface water reservoirs, underground mining, construction of tunnels, and detonation of underground explosions. Another type of induced seismicity that has attracted considerable public attention is fluid-induced seismicity, which involves injection or withdrawal of large volumes of fluids from the subsurface, including oil and gas production, disposal of brine or chemical waste, development of engineered geothermal systems or carbon sequestration. The underlying cause of injection-induced seismicity is understood to be a change in the state of stress acting on a pre-existing fault that leads to reduced clamping force or increased slip tendency. While there are examples of small earthquakes in western Canada induced by potash mining, most reported cases are fluid-induced. Cases considered here include small earthquakes up to about M4 from conventional hydrocarbon production, enhanced oil recovery, brine disposal and hydraulic fracturing. Fluid-induced seismicity is localized within a few specific areas (i.e. less than 1% of wells drilled are linked to induced seismicity), but more research is needed to fully understand the underlying risk factors and to calibrate ground-shaking models sufficiently for robust forecasting of specific scenarios. Risk management protocols have been introduced by regulators in some areas, through the implementation of traffic-light systems for hydraulic fracturing. While there have been economic consequences and public concern, to date these cases in western Canada have not resulted in any reported injuries. Learnings from this region may be valuable to inform public policy in other parts of the world.

1. INTRODUCTION

Induced seismicity refers to earthquakes or other seismic events that have a clear anthropogenic association. Human activities with potential to induce earthquakes include underground mining (Gibowicz and Kijko, 1994), construction of tunnels (Husen et al., 2013), impoundment of water reservoirs (Simpson et al., 1988), development of engineered geothermal systems (Breede et al., 2013), detonation of underground explosions (Massé, 1981) and subsurface fluid injection (Ellsworth, 2013) or extraction (Segall, 1989). There is growing recognition of the hazards posed by fluid-induced seismicity; examples of this category include saltwater disposal (SWD), CO_2 storage, enhanced oil recovery (EOR), and hydraulic fracturing (HF) (Figure 1).

The basic principles of fluid-induced seismicity have been understood for over five decades. A sequence of earthquakes from 1962 to 1968 near the Rocky Mountain Arsenal, Colorado provides a classic example of disposal-related seismicity. This sequence exhibited strong temporal correlation between injection and seismicity rates, as well as an approximately coplanar distribution of earthquake hypocentres in the basement close to the injection site (Healy et al., 1968). These observations prompted a subsequent experiment at the Rangely oil field in Colorado, where a multitude of small earthquakes occurred during waterflood operations (Raleigh et al., 1976). The Rangely experiment involved several cycles of raising and lowering of the reservoir pressure, whilst monitoring pressure in nearby wells along with seismic activity throughout the oil field. A pore pressure of ~ 26 MPa was found to be the activation threshold for seismicity.

Similarly, in western Canada, fluid-induced seismicity is not a new phenomenon (Figure 2). Induced seismicity has been observed since the mid 1970's in association with fluid injection or withdrawal. Early studies focused on seismic activity triggered by EOR near Fort St. John, B.C. (Horner et al., 1994) and gas production near Rocky Mountain House, Alberta (Baranova et al., 1999). More recent investigations have focused on persistent seismicity due to SWD within the Brazeau cluster in west central Alberta (Schultz et al., 2014), the Graham cluster in northeastern B.C. (BCOGC, 2014) and HF in various parts of the western Canada Sedimentary Basin (WCSB) (BCOGC, 2012, 2014; Atkinson et al., 2016; Schultz et al., 2017).

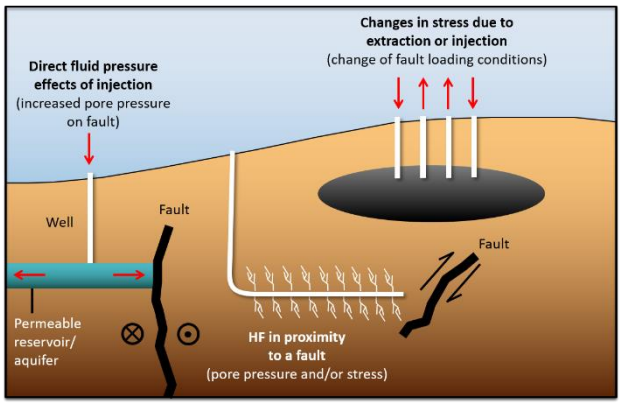

Figure 1. Schematic diagram showing mechanisms of fluid-induced seismicity. Modified from Eaton (2016).

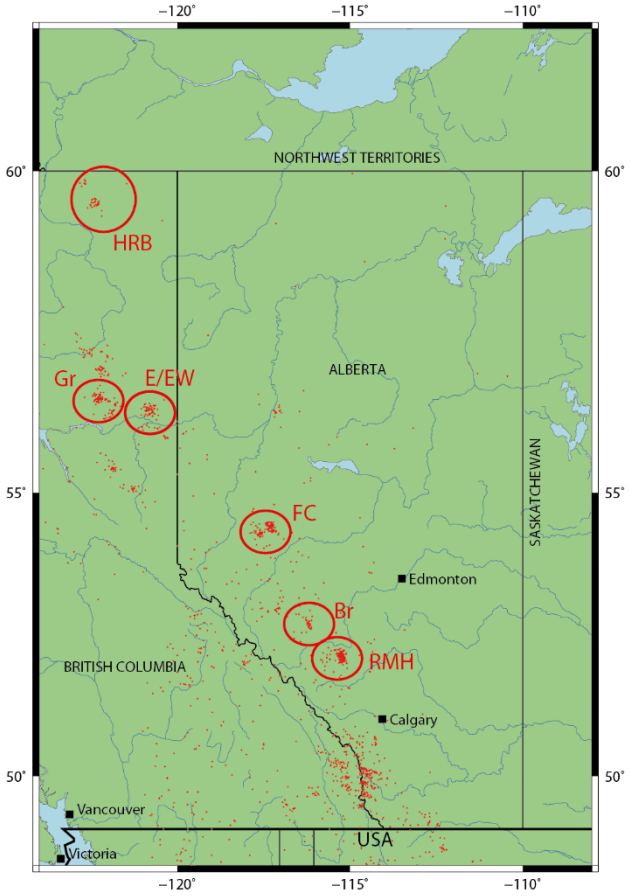

Figure 2. Map of western Canada showing historical recorded seismicity of M ≥ 2.5 up to 31 May 2017 from Fereidoni and Cui (2015). Clusters of induced seismicity discussed in this paper are circled: Br = Brazeau, E/EW = Eagle and Eagle West, FC = Fox Creek, Gr = Graham, HRB = Horn River Basin, and RMH = Rocky Mountain House.

The objectives of this paper are (1) to review key geomechanical concepts of induced seismicity; (2) to summarize, within this basic geomechanical framework, studies of induced seismicity in western Canada over the past few decades; (3) to discuss hypotheses for localized geological susceptibility to induced seismicity, and (4) to describe current strategies for management of risk from induced seismicity, including traffic light systems (Kao et al., 2016; 2018; Shipman et al, 2018) that have been recently introduced. In addition, we discuss factors that may impact maximum event magnitude, as well as the significance for ground motion of relatively shallow focal depths for induced seismic events.

2. BASIC GEOMECHANICS OF INDUCED SEISMICITY

The Mohr–Coulomb criterion is a linearized failure envelope that is widely used to represent conditions for frictional failure on a discontinuity, such as a fault or fracture (Figure 3). It can be expressed as

$$\tau = C + \mu(\sigma - \alpha P) \quad , \qquad [1]$$

where τ is the shear stress acting on the discontinuity, C is the cohesion, μ is the coefficient of static friction, σ is the normal stress, P is the pore pressure and α is Biot's parameter. The term $\sigma - \alpha P$ represents the effective stress, σ_{eff}. The fundamental role of pore pressure in reducing the frictional sliding resistance on a fault has been recognized since the concept of effective stress was introduced by King Hubbert and Rubey (1959).

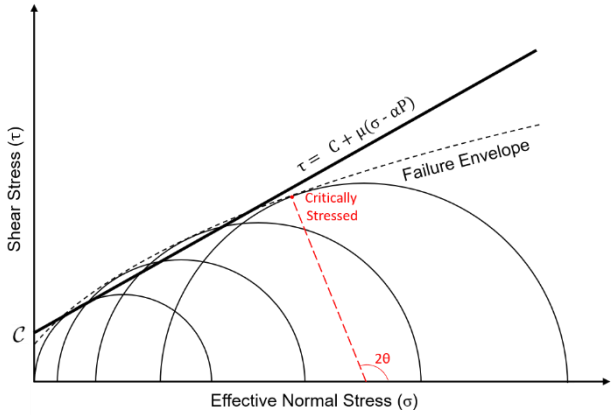

Figure 3. The Mohr–Coulomb failure criterion is a linearized form of the Mohr envelope, with slope defined by the coefficient of static friction (μ) and intercept defined by the cohesion, *C*. An example of a critically stressed fault is plotted. Modified from Eaton (2018).

A *critically stressed fault* is one that is in a state of incipient frictional failure (Zoback, 2010); in this state, a fault is subject to slip (failure) in response to a small perturbation in stress relative to the ambient stress field. The stress perturbation may be caused by either a decrease in effective stress, an increase in shear stress, or both.

A *favorably oriented fault* is characterized by a stress state that lies on (or above) the Mohr-Coulomb failure envelope (Figure 3). Depending on the coefficient of static friction, a favorably oriented fault typically has an inclination angle of about 30° between the fault plane and the plane containing the maximum and intermediate stress axes. Under steady-state conditions, Townend and Zoback (2000) proposed that large-scale stress feedbacks operate within the crust such that, as a general rule, favorably oriented faults are critically stressed.

Pore-pressure diffusion is a physical process, analogous to thermal diffusion, that causes pore pressure to spread from regions of relatively high pressure to regions of relatively low pressure. This process can occur in the absence of any bulk transport of pore fluid. It is thought to play an important role in fluid-induced seismicity by lowering the effective stress. Pore pressure diffusion can lead to a *triggering front* that marks the onset of an expanding cloud of induced seismicity (Shapiro and Dinske, 2009).

3. EXAMPLES FROM WESTERN CANADA

3.1 Production-related induced seismicity

A cluster of seismicity has been observed in the area southwest of Rocky Mountain House (Figure 2) since the mid-seventies (Baranova et al., 1999, Stern et al., 2013, Wetmiller, 1986). There appears to be a delayed correlation between gas production from the Strachan D3-A sour gas pool located in the region and the frequency of events. This pool targets a Devonian reef complex within the Leduc Formation. A total of 356 earthquakes were recorded from the mid-seventies to 2010 (Figure 4). The seismicity has gradually been declining as production slows. Since 2014, however, an uptick in the number of events has been observed, although production has remained stable. This uptick included a M4.3 event which was lightly felt by residents in Rocky Mountain House and tripped an electrical transformer, causing a power failure. Given the apparent lack of correlation with production trends from the Strachan D3-A pool, the triggering mechanism for this uptick in seismicity is currently unclear.

Segall (1989) showed that induced seismicity associated to fluid extraction can be modeled using the theory of poroelasticity, which implies that fluid extraction locally alters the state of stress. More specifically, the extraction of pore fluids results in localized contraction of the reservoir rocks, stressing and deforming the surrounding rock mass. This model is consistent with observations, as the seismicity in the Rocky Mountain House cluster is located below the reservoir (Wetmiller,1986). Moreover, in cases where earthquake mechanisms have been determined, they show reverse faulting, which fits well with the poroelastic model (Baranova et al., 1999; Segall, 1989). In this case, fluid extraction leads to contraction of the reservoir rock, which is accommodated by subsidence of the free surface: however, contraction in the horizontal direction is resisted, which causes the rock above and below the reservoir to be horizontally compressed. The a ~5-year delay between production and seismicity is accounted for in this model as the time necessary to accumulate the stresses required to initiate failure (Baranova et al., 1999). Once faults are activated, the coefficient of friction is lowered, bringing the Mohr-Coulomb failure criterion closer to the Mohr circle and leading to an increased correlation between production and seismicity.

3.2 Enhanced Oil Recovery (EOR)

The first earthquakes in the Eagle and Eagle West field cluster (Figure 2) were observed in 1984 (Figure 5), despite monitoring capabilities in the region since the mid-sixties (Horner et al., 1994). Unfortunately, the available hypocenter accuracy at the time was low due to the sparse monitoring network. Despite this, there appears to be an obvious spatial correlation with the Eagle West and Eagle oil fields. Early earthquakes are located close to Eagle West, while the earthquakes from 1992-1993, and perhaps even as early as 1986, are located further east in the Eagle field. Nineteen of the 24 total events can be grouped into 3 distinct clusters lasting for approximately one month, suggesting a relationship similar to a mainshock-aftershock sequence. The largest event magnitude was around M4.3.

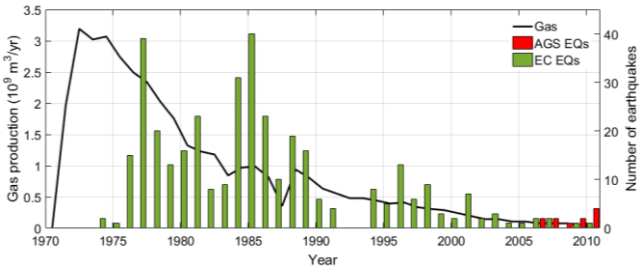

Figure 4. Histograms of number of earthquakes recorded within 40 km of the Strachan D3-A Pool near Rocky Mountain House from Earthquake Canada (EC) and Alberta Geological Survey (AGS) catalogues, and compared to the yearly gas production. Adapted from Stern et al. (2013).

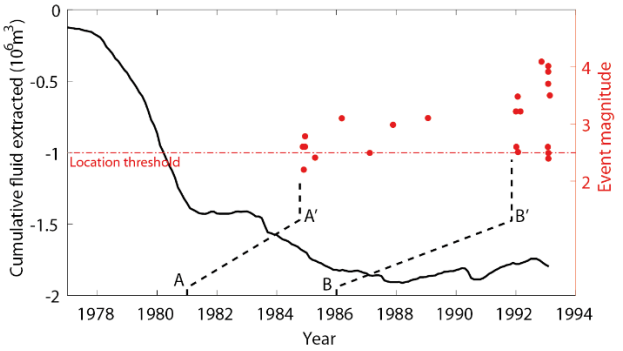

Figure 5. Combined cumulative fluid extracted from the Eagle West and Eagle reservoirs from January 1977 to March 1993 (black), and the observed seismicity (red). A-A' and B-B' indicate the commencement of EOR in the Eagle West and Eagle fields, respectively. Seismicity in the Eagle field may have begun as early as 1986. Adapted from Horner et al. (1994).

The Eagle and Eagle West pools were initially produced by solution gas drive (expansion of the oil and dissolved solution gas in response to pressure released at the surface), reducing reservoir pressures by up to 50 %. This was inefficient, so EOR by water injection was introduced at Eagle West in 1980, and Eagle in 1985 (Figure 5). The cumulative fluid extracted (total volume extracted minus that injected) is shown in Figure 5 and appears to show no correlation with the seismicity. However, the initiation of EOR does appear to relate with seismicity, albeit with a delay of 4–6 years. This may be related to the time required for pressure diffusion through the reservoir to initiate slip on optimally oriented pre-existing faults. Another possible factor may be an increase in surface injection pressure, which for Eagle West increased from 20 MPa to 23 MPa in 1984, around the time of the first seismicity. Using

estimated regional stresses, Horner et al. (1994) demonstrated that the injection pressures are sufficient to cause the failure envelope to intersect the Mohr circle for the reservoir.

Although there was a lack of seismicity before EOR, there is abundant evidence for faults in the region (Horner et al., 1994). This area is situated in the Fort St. John graben and has experienced episodic tectonic activity since at least the Proterozoic. There are numerous high-angle basement-rooted faults in the region, and the Eagle and Eagle West fields are located in one of the more tectonically active regions of the Arch, on the north rim of the Fort St. John graben. This association with pre-existing faults likely increases the local geological susceptibility to induced seismicity.

3.3 Saltwater Disposal (SWD)

As of 2014, only two of 104 active wastewater disposal wells in British Columbia (BC) had been linked to induced seismicity (BCOGC, 2014). One of these is at the Graham pool (Figure 2), where over 122 events with magnitudes up to ~M4.0 have been detected and associated with a deep wastewater disposal well (BCOGC, 2014). These events began 13 months after the initiation of disposal. No injuries or damage have been linked to this event sequence. It is believed that this region is particularly susceptible to induced seismicity due to its location in the Rocky Mountain foothills belt, close to the pre-existing structures of the Fort St. John Graben complex, similarly to the Eagle and Eagle West fields (section 3.2).

Schultz et al. (2014) described the relationship between a wastewater injection well in the Brazeau region, Alberta (Figure 2) and a disposal well in the Cordel field. They found a statistically significant increase in seismicity which lagged the onset of wastewater injection in 1991 by ~3.3 years. This delay is attributed to the time necessary for pore-pressure diffusion to reach the pre-existing fracture network, and the time required for the buildup of pressure required to exceed the Mohr-Coulomb failure threshold. Events show significant waveform similarity, suggesting that they have similar locations and mechanisms, and allowing for a double difference relocation method to be performed (Figure 6). Hypocenters trend along an approximately N-S oriented linear feature that dips at an angle of 35° to a maximum depth of 9 km, well within the Precambrian basement.

3.4 Hydraulic Fracturing

In the case of hydraulic fracturing (HF), fluids are injected under high pressure during well completion to produce local fractures within the rock, increasing permeability in low permeability unconventional reservoirs to allow for hydrocarbon extraction (Eaton, 2018). The first reported case of HF induced seismicity was in 2010 near Blackpool, UK, and had a magnitude of M2.3 (Grigoli et al., 2017). Since then, a large number of seismic events have been attributed to HF. This is especially the case in western Canada, where the majority of recent induced events are highly correlated in time and space with HF (Atkinson et al., 2016). The occurrence of these events is mostly limited to four main regions: the Horn River Basin (HRB), the Montney play in BC, southern Alberta, and the Fox Creek area of west central Alberta. Each of these regions will be discussed in turn.

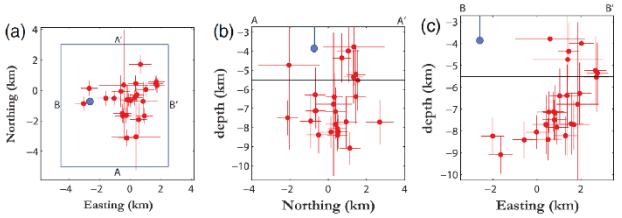

Figure 6. Robust double difference relocations of events (red crosses) from the Brazeau cluster, in (a) map view (blue circle = disposal well), (b) S-N cross-section, and (c) W-E cross-section. The span of event cross hairs indicates 90 % confidence intervals in locations, and the approximate Precambrian basement depth is shown in black. Reproduced from Schultz et al. (2014).

The HRB, northeast BC (Figure 2), is one of the largest shale gas regions in North America (Farahbod et al., 2015a). It consists of three organic-rich formations of Devonian age: the Evie, Otter Park and Muskwa Formations (Harris and Dong, 2013). A major N-S fault system, the Bovie fault, separates the HRB from the neighbouring Liard Basin to the west.

Large-scale shale gas production was first developed in the HRB in 2006 (BCOGC, 2012), and became more widespread from 2009-2011 (Farahbod et al., 2015a). Very few earthquakes were reported until 2010 (Farahbod et al., 2015a; 2015b). As the scale of HF operations increased from late 2006 to 2011, the level of local seismicity also clearly increased, both in number and magnitude, with 40 earthquakes reported by Natural Resources Canada from 2009 up to mid-2014. Taking the HRB as a whole, Farahbod et al. (2015b) suggested that the increasing seismicity is related to the volume of fluid injected, and not to the injection pressures used. No clear change in seismicity is observed when the total monthly injected volume is < 20,000 m^3. Relatively large seismic moment events (> 10^{14} Nm) are only observed when that rate exceeds 150,000 m^3. In a similar manner to other types of induced seismicity, variable time lags of days to months are observed between HF operations and significant earthquakes.

HF induced seismicity has also been observed in the Montney play in northeast BC (BCOGC, 2014; Mahani et al., 2017), in the region around the previously discussed Eagle, Eagle West and Graham areas (Figure 2). The seismicity is predominantly located within the deformed Rocky Mountain foothills belt and structures of the Fort St. John Graben complex (BCOGC, 2014). Development of Montney unconventional siltstone units began in about 2005. The number of M ≥ 3 events increased threefold from 33 in 2008 to 97 in 2015, and these events have been

statistically correlated with an increase in HF operations in the area (Mahani et al., 2017). The depths of many of these events have been located at 0.5 to 2.5 km depth, which lies above the target zone where HF was taking place (Mahani et al., 2017). The largest event was a M4.6, one of the largest in the world to be associated with HF. The mechanism of this event was found to be thrust faulting, consistent with the compressional stress regime of the region (Mahani et al., 2017).

tensor inversion has revealed normal slip, consistent with stress data for the area. Schultz et al. (2015a) concluded that the events were likely triggered due to increased pore pressure on a pre-existing basement fault.

More recently, a great deal of attention has been given to swarms of seismicity generated by hydraulic fracturing operations in the Duvernay play of central Alberta, which is composed of a prolific organic-rich mudstone source rock

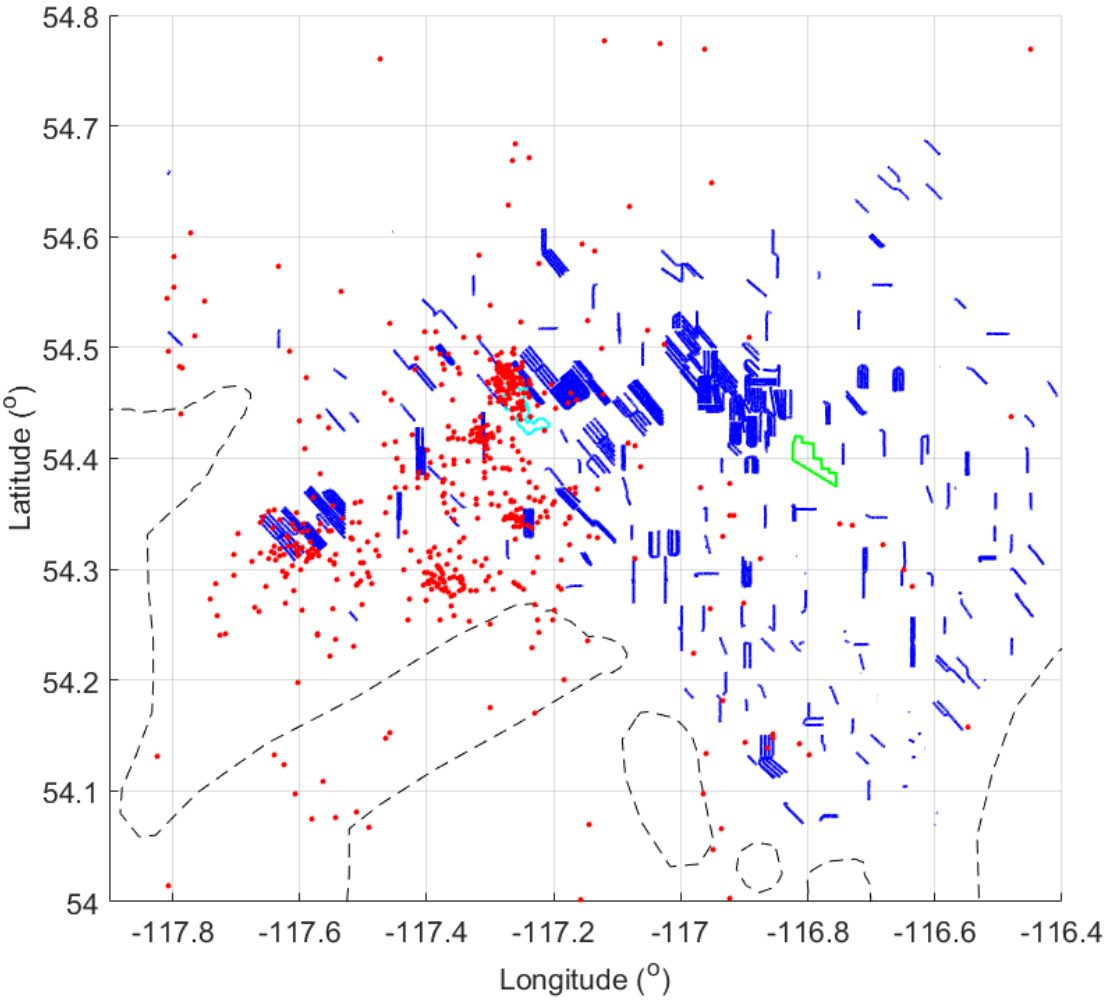

Figure 7. Map of the Fox Creek region of central Alberta, showing hydraulic fracturing wells targeting the Duvernay Formation (blue) and seismicity from Stern et al. (2017) (red). Also shown are Fox Creek town boundaries (green), Crooked Lake (cyan) and the inferred border between the Duvernay Formation and fossil reef structures (black dashed).

In Alberta, the first seismicity attributed to HF was the Cardston swarm, located close to the US border (Schultz et al., 2015a). More than 60 earthquakes with M0.7-3.0 were detected from December 2011 to March 2012, in an area with little evidence for previous seismicity. The timing of the events is strongly correlated to hydraulic fracturing operations at a nearby horizontal HF well (> 99.7 % confidence). Events show strong waveform similarity suggesting similar locations and mechanisms, and are likely located within the crystalline basement. Moment

interfingered with impermeable limestone (Bao and Eaton, 2016). Although the play extends for over 400 km, induced seismicity has been concentrated in the region west of the town of Fox Creek (Figure 2), close to Crooked Lake, where a number of events with M ≥ 3 have been recorded. A M3.9 event on 23 January 2015 prompted a significant regulatory response, namely the introduction of a “traffic light protocol” (TLP) in Alberta (Shipman et al., 2018). The TLP mandates an immediate shutdown of HF operations following an earthquake of local magnitude ≥ 4.0, and reporting of events of magnitude ≥ 2.0 (Schultz et al.,

2017). Induced seismicity was first identified in the area in late 2013 (Schultz et al., 2015b), although HF operations had been active in the area since June 2010 (Schultz et al., 2017). The locations of earthquakes recorded in the region by the Alberta Energy Regulator are shown in Figure 7, as well as the locations of HF wells targeting the Duvernay Formation. Most of the events are correlated spatially and temporally with HF treatments. However, the seismicity appears to cluster close to and west of Crooked Lake, despite a large number of completions in other areas. This suggest that there are geological controls on the occurrence of seismicity in the region. Schultz et al. (2016) suggested that one of these controls may be the proximity of the wells to fossil reef margins; this association has been supported by findings of Pawley et al. (2018) using a machine learning algorithm. Two arguments are given for this potential link: (1) reef growth may have nucleated on elevated structures associated with basement tectonics, and (2) these structures may allow for hydraulic communication between strata. In Figure 7, events are observed for many of the HF treatments located close to the reef edges (Schultz et al., 2016).

High-resolution monitoring in this region has allowed studies to map clusters of seismicity associated with individual treatments. Bao and Eaton (2016) studied a sequence of events including a M3.9 event which occurred several weeks after the related injection. The seismicity appears to delineate two N-S striking, subvertical faults that extend from the injection zone into the crystalline basement where the large event occurred. Bao and Eaton (2016) found that the east fault strand was most likely triggered by stress changes due to injection, while the west strand, which exhibited longer-lived seismicity, was more likely triggered by pore-pressure changes.

Another study by Eyre et al. (2018) utilized a dense, shallow borehole monitoring network of a HF treatment in 2016, allowing for a magnitude of completeness of events of M –2.0. This treatment was associated with a M4.1 event, one of the largest to be observed in the Fox Creek region. Over 9,000 events were detected, most clustering along subvertical linear structures striking N-S to NNE-SSW (Figure 8). Along with strike-slip source mechanisms obtained for this and other datasets in the region (Eyre et al., 2018; Wang et al., 2016; Wang et al., 2017), the pattern suggests a complex flower structure and is consistent with the regional stress regime. Eyre et al. (2018) conclude that the events are most likely pore-pressure induced, and the N-S well orientation was “optimally” oriented to produce the large number of events observed. Another interesting finding, in comparison to the findings of Bao and Eaton (2016), is that the majority of the events are located above the target formation, including the M4.1 event. The location above the target zone is a robust result, as the perforation shots from the treatment with known locations were detected and used to calibrate the seismic velocity model (Eyre et al., 2018).

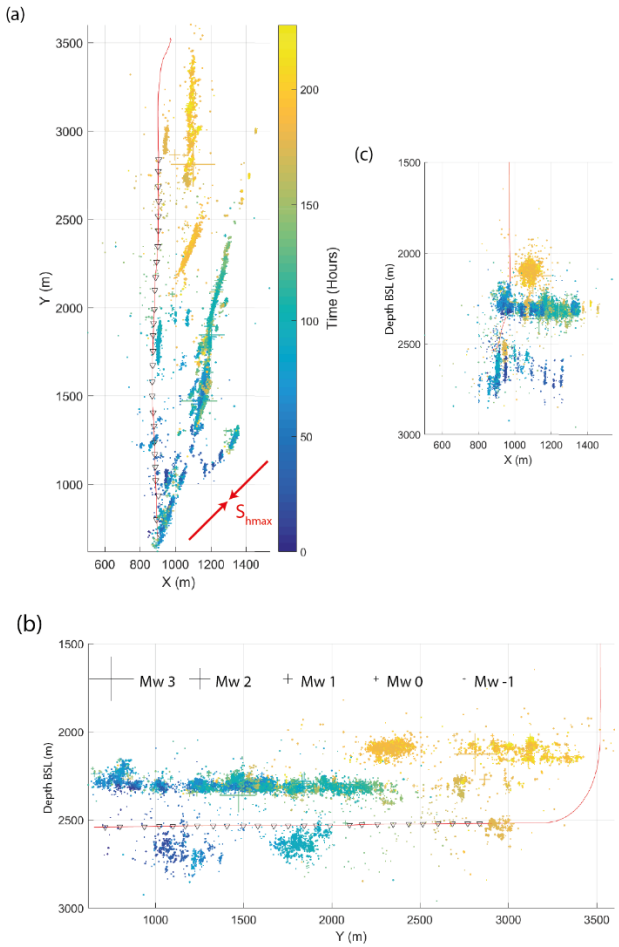

Figure 8. Location results for 9,769 events associated with a hydraulic fracturing treatment, in (a) map view, (b) S-N cross-section, and (c) W-E cross-section, and coloured by time. Marker size is exponentially scaled by magnitude, and treatment well (red) and stages (triangles) are shown. Modified from Eyre et al. (2018).

More recent work focused on the Fox Creek region has worked to identify the injection parameters most closely associated with induced seismicity in the Duvernay. Schultz et al. (2018) showed that induced earthquakes are associated with larger injection volumes (10^4 to 10^5 m^3) and that seismic productivity scales linearly with injection volume, while injection pressure and rate show negligible correlation. However, geological factors are also believed to play a prominent role. Volume and geological factors are estimated to account for 96% of the variability in induced earthquake rate near Fox Creek (Schultz et al., 2018). Another study looked to identify any specific geological bias in seismogenic activation potential which appears to control the distribution of earthquakes. Pawley et al. (2018) use a machine learning algorithm to systematically evaluate parameters suspected to control induced seismicity. They determined that the most important parameters are proximity to basement, in situ stress, proximity to fossil reef margins, lithium concentration and rate of natural seismicity.

4. DISCUSSION

Induced seismicity in western Canada has been caused by a number of anthropogenic processes involving fluid injection or extraction, i.e. hydrocarbon production, EOR, SWD and HF. However, induced seismicity associated with any of these processes is rare, and limited to small clusters of events (Figure 2). Atkinson et al. (2016) showed that, for the period 1985-2015, only ~1 % of disposal wells were associated with seismicity with M ≥ 3, and for HF this percentage was even smaller (~0.3 %) (Table 1). Therefore, the vast majority of HF, SWD and other operations have no associated induced seismicity. Despite this, induced seismicity formed 93 % of all seismicity in the WCSB between 2010 and 2015 (Table 1), and has therefore been a highly significant hazard in recent years which will likely continue into the future. Thankfully, due to the sparse populations in the regions where induced seismicity has been observed, no injuries and little damage have been reported thus far.

What is evident from these findings and the clustering of induced seismicity is that geological susceptibility plays a key role in whether induced seismicity is likely to occur in a region. In NE BC, many of the seismicity clusters are located in the Rocky Mountain foothills belt close to or within the Fort St John Graben complex, a significant highly-faulted tectonic structure (Horner et al., 1994). The appearance of these clusters of events suggests that this structure is close to critical stress in at least some places. In Alberta, the reasons behind geological susceptibility are less clear as most of the events occur in regions previously believed to be tectonically inactive. As discussed in section 3.4, Schultz et al. (2016) proposed that the susceptibility in this region may be linked to the locations of fossil reef structures. Further work by Pawley et al. (2018) showed that this may be one of a number of factors influencing the locations of induced seismicity, with others including proximity to basement, reservoir pressure, minimum horizontal stress and reservoir thickness. Another necessary criterion is likely the presence of pre-existing critically stressed faults (Eaton and Igonin, 2018). Mapping of pre-existing faults would be highly desirable, however in many regions it is not possible as many of them cannot be robustly detected by current imaging methods such as 3D seismic surveys (Eaton and Igonin, 2018; Eyre et al., 2018). It therefore seems that the geological susceptibility is a highly complex parameter, and further work is required to gain a better understanding of why some regions are more prone to induced seismicity than others.

Currently, the WCSB appears to be unique in that most of the induced seismicity is associated with hydraulic fracturing (Table 1). In contrast, in the USA the majority of induced seismicity has been attributed to SWD (Ellsworth, 2013). However, since the discovery of HF induced earthquakes in Canada, HF induced seismicity has been identified in many of the major shale plays in the USA, with published examples including Ohio (Skoumal et al., 2015) and Arkansas (Yoon et al., 2017). Findings from the WCSB could be vital for mitigation of this seismicity.

Table 1. Summary of seismicity M ≥ 3 associated with wells in the western Canada sedimentary basin (from Atkinson et al., 2016).

	Disposal	HF	Tectonic
# of candidate wells (1985-2015)	1236	12,289	-
# of wells associated with M ≥ 3	17	39	-
Association % for wells	~1 %	~0.3 %	-
# of M ≥ 3 (1985-2009)	126*	13*	14
# of M ≥ 3 (2010-2015)	33*	65*	7
Association % for M ≥ 3 (2010-2015)	31 %	62 %	7 %

*Totals include 18 events for which both disposal and HF wells could be associated (8 from 2010-2015): each such event has been counted as ½.

Current mitigation strategies in the WCSB are based on the use of traffic light protocols. Regulators in both BC and Alberta have adopted various aspects as part of their individual oversight and mitigation strategies (Kao et al., 2016; 2018). In both cases, the red-light threshold is set at local magnitude 4.0, which appears to be adequate in characterizing the potential seismic risk. The yellow-light threshold in Alberta is local magnitude 2.0. From the introduction of the protocols in 2014 up until early 2018, three red light events occurred each in BC and Alberta, respectively. All events in Alberta were preceded by a yellow event, while only one in BC was preceded by an event in that magnitude range (Kao et al., 2018). One issue that has been observed since the introduction of traffic light protocols in western Canada is that, once an earthquake sequence is induced, events often continue after HF is completed. Another issue that has arisen involves uncertainty in magnitude calculation. Kao et al. (2018) made some suggestions for improvement, such as incorporating ground motion information, standardizing magnitude calculations, and adapting the traffic light protocol to local hazard conditions.

Another aspect of mitigating induced seismicity is forecasting consideration of factors that could influence the maximum magnitude of induced events. In principle, using basic concepts from earthquake seismology, i.e. the equations of Kanamori and Anderson (1975), fault size could be used to constrain the maximum estimated magnitude for an induced event (Eaton and Igonin, 2018). In such a scheme, only faults that are in sufficiently close proximity to an injection site and are favorably oriented for reactivation in the ambient stress field would need to be considered (Walsh and Zoback, 2016). However, in practice, such an approach is not feasible, chiefly because of daunting challenges in identifying and mapping all potentially seismogenic faults, in view of the likely situation that many faults that can be detected may not be seismogenic (Eaton and Igonin, 2018).

Alternative approaches have focused on the statistical characteristics of seismicity. Eaton and Igonin (2018) give an overview of the three common methods for calculating maximum magnitude of induced seismicity and test them using data from western Canada. Model 1, Shapiro's hypothesis (Shapiro et al., 2011), postulates that the fault rupture area is entirely contained within the stimulated reservoir volume, and therefore the maximum magnitude is constrained by an expanding pore pressure diffusion front. Model 2, McGarr's hypothesis (McGarr, 2014), expresses the maximum seismic moment (M_0(max)) in terms of the net injected fluid volume ΔV:

$$M_0(\max) = \mu \Delta V, \quad [2]$$

where μ is the shear modulus of the medium. Model 3, van der Elst's hypothesis (van der Elst et al., 2016), postulates that observed maximum magnitudes correspond to the statistical expectation for a finite sample of events, which assuming an unbounded Gutenberg-Richter distribution is dependent on the *b*-value and the number of detected events *N*. Van der Elst et al. (2016) further link their model to net injected volume *V* using the concept of seismogenic index, Σ (Shapiro et al., 2010):

$$\Sigma = \log_{10} N - \log_{10} V + bM_r, \quad [3]$$

where M_r is the reference magnitude (often magnitude of completeness). With this they derive an alternative formula for maximum magnitude (M_{max}):

$$M_{max} = \frac{1}{b}(\Sigma + \log_{10} V). \quad [4]$$

Each of these models has implications for hazard mitigation strategies such as traffic light protocols. For example, for model 1 monitoring the expanding microseismic cloud could be used to manage the maximum magnitude. Models 2 and 3 appear to be more consistent with induced seismicity observations elsewhere in the world (McGarr, 2014; van der Elst et al., 2016). In western Canada, studies such as Schultz et al. (2018) show a link between injected volumes and induced seismicity, and therefore it would be expected that these models should also perform well here.

Induced seismicity from HF in western Canada, however, does not conform exactly any of these models (Eaton and Igonin, 2018). Model 3 may be adapted by changing the seismogenic index within susceptible regions; however, *a priori* knowledge of seismogenic index is not well constrained for most areas and therefore the model is difficult to implement. Another possibility is that the maximum magnitude of these HF induced events is solely controlled by the fault area. If so, further research is needed to improve methods to identify and map potentially seismogenic faults.

Induced earthquakes tend to have shallower focal depths than natural events from the same region (Zhang et al., 2016). All else being equal, this relationship supports a general expectation that ground shaking intensity close to the epicenter should be greater in the case of induced earthquakes than that for a natural earthquake, owing to closer proximity of the source. There is evidence, however, that for a given magnitude the ground-shaking from induced earthquakes may be systematically lower than expected, based on ground-motion relationships derived from natural seismicity (Hough, 2014). This finding could be explained if the stress drop (co-seismic stress change on a fault) were lower for induced earthquakes (Hough, 2014), although this generalization is not supported by stress-drop observations in western Canada (Zhang et al., 2016). A recent study of earthquakes in Oklahoma (Atkinson et al., 2018) finds that induced and natural earthquakes of the same magnitude have similar average intensities within 10 km of the epicenter, whereas the average intensity of induced events is less than natural events at greater distances. This relationship is inferred to be due to the generally shallower focal depths of induced events, which is offset by the general increase in stress drop with depth (Atkinson et al., 2018).

5. Conclusions

Induced seismicity in western Canada is mostly fluid-induced, and > 66 % is related to HF. However, although significant, less than 1 % of HF and injection wells are associated with seismicity. For HF, there appears to be a relationship between volume of injected fluid and the induced seismicity produced. However, all induced seismicity seems to be strongly dependent on the geological susceptibility of the region to hydraulic fracturing, and most of the induced seismicity appears in confined clusters. Mitigation by the regulators has focused on traffic light protocols which have been somewhat successful in reducing hazard. However, forecasting maximum magnitudes has proved difficult for HF induced events as the largest event magnitudes often exceed model predictions. Findings from western Canada could be vital for the mitigation of induced seismicity in other areas throughout the world, especially that related to HF.

6. Acknowledgements

The authors with to thank Repsol Oil & Gas Canada Inc. for providing the data used in Figure 8. The data used in Figure 8 were processed by Magnitude. This review was undertaken thanks in part to funding from the Canada First Research Excellence Fund.

7. References

Atkinson, G. M., Eaton, D. W., Ghofrani, H., Walker, D., Cheadle, B., Schultz, R., Shcherbakov, R., Tiampo, K., Gu, Y. J., Harrington, R. M., Liu, Y., Van der Baan, M., and Kao, H. 2016. Hydraulic fracturing and seismicity in the Western Canada Sedimentary Basin. *Seismological Research Letters*, 87: 631–647.

Atkinson, G.M., Wald D. C., Worden, B. and Quitoriano, V., 2018. The Intensity Signature of Induced Seismicity. Bulletin of the Seismological Society of America, DOI: https://doi.org/10.1785/0120170316.

Bao, X., and Eaton, D.W. 2016. Fault activation by hydraulic fracturing in western Canada. *Science*, 354, 1406-1409.

Baranova, V., Mustaqeem, A., and Bell, S. 1999. A model for induced seismicity caused by hydrocarbon production in the Western Canada Sedimentary Basin. *Canadian Journal of Earth Sciences*, 36: 47–64.

BCOGC. 2012. Investigation of Observed Seismicity in the Horn River Basin. Tech. Report, BC Oil & Gas Commission. https://www.bcogc.ca/node/8046/download

BCOGC. 2014. Investigation of Observed Seismicity in the Montney Trend. Technical Report, BC Oil & Gas Commission: https://www.bcogc.ca/node/12291/download

Breede, K., Dzebisashvili, K., Liu, X., and Falcone, G. 2013. A systematic review of enhanced (or engineered) geothermal systems: Past, present and future. *Geothermal Energy*, 1: 4. https://doi.org/10.1186/2195-9706-1-4.

Eaton, D.W., 2016. Injection-induced seismicity: An academic perspective. CETI Journal, 2(4), 34–41.

Eaton, D.W. 2018. Passive seismic monitoring of induced seismicity: Fundamental principles and application to energy technologies. *Cambridge University Press*, in press.

Eaton, D.W., and Igonin, N. 2018. What controls the maximum magnitude of injection-induced earthquakes? *The Leading Edge*, 37(2), 135-140.

Ellsworth, W. L. 2013. Injection-induced earthquakes. *Science*: 341, 1225942.

Eyre, T.S., Eaton, D.W., D'Amico, D., Kolos, D., and Zecevic, M. 2018. Microseismicity reveals fault activation before M_w 4.1 hydraulic-fracturing induced earthquake. *Bulletin of the Seismological Society of America*, in review.

Farahbod, A.M., Kao, H., Walker, D.M., and Cassidy, J.F. 2015a. Investigation of regional seismicity before and after hydraulic fracturing in the Horn River Basin, northeast British Columbia. *Canadian Journal of Earth Sciences*, 52(2): 112-122.

Farahbod, A.M., Kao, H., Cassidy, J.F., and Walker, D. 2015b. How did hydraulic-fracturing operations in the Horn River Basin change seismicity patterns in northeastern British Columbia, Canada? *The Leading Edge*, 34(6): 658-663.

Fereidoni, A., and Cui, L., 2015. Composite Alberta Seismicity Catalog. *http://www.inducedseismicity.ca/catalogues/*

Gibowicz, S. J., and Kijko, A. 1994. *An Introduction to Mining Seismology*. Academic Press.

Grigoli, F., Cesca, S., Priolo, E., Rinaldi, A.P., Clinton, J.F., Stabile, T.A., Dost, B., Fernandez, M.G., Wiemer, S., and Dahm, T. 2017. Current challenges in monitoring, discrimination, and management of induced seismicity related to underground industrial activities: a European perspective. *Reviews of Geophysics*, 55, 310-340.

Harris, N.B., and Dong, T. 2013. Characterizing porosity in the Horn River shale, northeastern British Columbia. *Geoscience Reports 2013*, *British Columbia Ministry of Natural Gas Development*, 33-40.

Healy, J. H., Rubey, W. W., Griggs, D. T., and Raleigh, C. B. 1968. The Denver earthquakes. *Science*, 161: 1301–1310.

Horner, R.B., Barclay, J.E. and Macrae, J.M. 1994. Earthquakes and Hydrocarbon Production in the Fort St. John Area of Northeastern B.C. *Canadian Journal of Exploration Geophysics*, 30: 39-50.

Hough, S.E. 2014. Shaking from injection-induced earthquakes in the central and eastern United States. *Bulletin of the Seismological Society of America*, 104(5), 2619-2626.

Husen, S., Kissling, E., and von Deschwanden, A. 2013. Induced seismicity during the construction of the Gotthard Base Tunnel, Switzerland: Hypocenter locations and source dimensions. *Journal of Seismology*, 17: 63–81.

Kanamori, H., and Anderson, D.L. 1975. Theoretical basis of some empirical relations in seismology. *Bulletin of the Seismological Society of America*, 65, 1073-1095.

Kao, H., Eaton, D. W., Atkinson, G. M., Maxwell, S., and Mahani, A. B. 2016. *Technical Meeting on the Traffic Light Protocols (TLP) for Induced Seismicity: Summary and Recommendations*. Open File Report 8075. Geological Survey of Canada.

Kao, H., Visser, R., Smith, B., and Venables, S. 2018. Performance assessment of the induced seismicity traffic light protocol for northeastern British Columbia and western Alberta. *The Leading Edge*, 37(2), 117-126.

King Hubbert, M., and Rubey, W.W. 1959. Role of fluid pressure in mechanics of overthrust faulting. *Bulletin of the Geological Society of America*, 70: 115-166.

Mahani, A.B., Schultz, R., Kao, H., Walker, D., Johnson, J., and Salas, C. 2017. Fluid injection and seismic activity in the northern Montney play, British Columbia, Canada, with special reference to the 17 August 2015 M_w 4.6 induced earthquake. *Bulletin of the Seismological Society of America*, 107(2): 542-552.

Massé, R. P. 1981. Review of seismic source models for underground nuclear explosions. *Bulletin of the Seismological Society of America*, 71: 1249–1268.

McGarr, A. 2014. Maximum magnitude earthquakes induced by fluid injection. *Journal of Geophysical Research: Solid Earth*, 119(2), 1008–1019.

Pawley, S., Schultz, R., Playter, T., Corlett, H., Shipman, T., Lyster, S., and Hauck, T. 2018. The geological susceptibility of induced earthquakes in the Duvernay play. *Geophysical Research Letters*, 45, accepted.

Raleigh, C. B., Healy, J. H., and Bredehoeft, J. D. 1976. An experiment in earthquake control at Rangely, Colorado. *Science*, 191: 1230–1237.

Schultz, R., Stern, V., and Gu, Y. J. 2014. An investigation of seismicity clustered near the Cordel Field, west central Alberta, and its relation to a nearby disposal well. *Journal of Geophysical Research: Solid Earth*, 119: 3410–3423.

Schultz, R., Mei, S., Pană, D., Stern, V., Gu, Y.J., Kim, A., and Eaton, D.W. 2015a. The Cardston earthquake swarm and hydraulic fracturing of the Exshaw Formation (Alberta Bakken play). *Bulletin of the Seismological Society of America*, 105(6): 2871-2884.

Schultz, R., Stern, V., Novakovic, M., Atkinson, G., and Gu, Y.J. 2015b. Hydraulic fracturing and the Crooked Lake sequences: insights gleaned from regional seismic networks. *Geophysical Research Letters*, 42: 2750-2758.

Schultz, R., Corlett, H., Haug, K., Kocon, K., MacCormack, K., Stern, V., and Shipman, T. 2016. Linking fossil reefs with earthquakes: geologic insight to where induced seismicity occurs in Alberta. *Geophysical Research Letters*, 43: 2534-2542.

Schultz, R., Wang, R., Gu, Y. J., Haug, K., and Atkinson, G. M. 2017. A seismological overview of the induced earthquakes in the Duvernay play near Fox Creek, Alberta. *Journal of Geophysical Research: Solid Earth*, 122: 492–505.

Schultz, R., Atkinson, G., Eaton, D.W., Gu, Y.J., and Kao, H. 2018. Hydraulic fracturing volume is associated with induced earthquake productivity in the Duvernay play. *Science*, 359, 304-308.

Segall, P. 1989. Earthquakes triggered by fluid extraction. *Geology*, 17: 942-946.

Shapiro, S. A. 2015. *Fluid-Induced Seismicity*. Cambridge University Press.

Shapiro, S.A., and Dinske, C. 2009. Fluid-induced seismicity: Pressure diffusion and hydraulic fracturing. *Geophysical Prospecting*, 57: 301-310.

Shapiro, S. A., Dinske, C., Langenbruch, C., and Wenzel, F. 2010. Seismogenic index and magnitude probability of earthquakes induced during reservoir fluid stimulations. *The Leading Edge*, 29(3), 304–309.

Shapiro, S.A., Krüger, O.S., Dinske, C., and Langenbruch, C. 2011. Magnitudes of induced earthquakes and geometric scales of fluid-stimulated rock volumes. *Geophysics*, 76(6), WC55–WC63.

Shipman, T., MacDonald, R. and Byrnes, T. 2018. Experiences and learnings from induced seismicity regulation in Alberta. *Interpretation*, 6(2), SE15-SE21.

Simpson, D. W., Leith, W. S., and Scholz, C. H. 1988. Two types of reservoir-induced seismicity. *Bulletin of the Seismological Society of America*, 78: 2025–2040.

Skoumal, R.J., Brudzinski, M.R., and Currie, B.S. 2015. Induced earthquakes during hydraulic fracturing in Poland Township, Ohio. *Bulletin of the Seismological Society of America*, 105(1): 189-197.

Stern, V.H., Schultz, R.J., Shen, L., Gu, Y.J., and Eaton, D.W. 2013. Alberta Earthquake Catalogue, Version 1.0: September 2006 through December 2010. *Alberta Energy Regulator*, *AER/AGS Open File Report 2013-2015*, 29 p.

Stern, V.H., Schultz, R.J., Shen, L., Gu, Y.J., and Eaton, D.W. 2017. Alberta Earthquake Catalogue, Version 5.0: (GIS data, point features). *Alberta Energy Regulator*, *AER/AGS Digital Dataset 2013-0017*.

Townend, J., and Zoback, M. D. 2000. How faulting keeps the crust strong. *Geology*, 28: 399–402.

van der Elst, N.J., Page, M.T., Weiser, D.A., Goebel, T.H.W., and Hosseini, S.M. 2016. Induced earthquake magnitudes are as large as (statistically) expected. *Journal of Geophysical Research: Solid Earth*, 121(6), 4575–4590.

Walsh, F.R. III, and Zoback, M.D. 2016. Probabilistic assessment of potential fault slip related to injection-induced earthquakes: Application to north-central Oklahoma, USA. *Geology*, 44(12), 991–994.

Wang, R., Gu, Y.J., Schultz, R., Kim, A., and Atkinson, G. 2016. Source analysis of a potential hydraulic fracturing induced earthquake near Fox Creek, Alberta. *Geophysical Research Letters*, 43(2), 564-573.

Wang, R., Gu, Y.J., Schultz, R., Zhang, M., and Kim, A. 2017. Source characteristics and geological implications of the January 2016 induced earthquake swarm near Crooked Lake, Alberta. *Geophysical Journal International*, 210(2), 979-988.

Wetmiller, R.J. 1986. Earthquakes near Rocky Mountain House, Alberta, and their relationship to gas production facilities. *Canadian Journal of Earth Sciences*, 23: 172-181.

Yoon, C.E., Huang, Y., Ellsworth, W.L., and Beroza, G.C. 2017. Seismciity during the initial stages of the Guy-Greenbrier, Arkansas, earthquake sequence. *Journal of Geophysical Research: Solid Earth*, 122, 9253-9274.

Zhang, H., Eaton, D.W., Li, G., Liu, Y. and Harrington, R.M. 2016. Discriminating induced seismicity from natural earthquakes using moment tensors and source spectra. *Journal of Geophysical Research: Solid Earth*, 121(2), 972-993.

Zoback, M. D. 2010. *Reservoir Geomechanics*. Cambridge University Press.